

Linear optical response of metallic nanoshells in different dielectric media

O. Peña,¹ U. Pal,^{1,*} L. Rodríguez-Fernández,² and A. Crespo-Sosa²

¹*Instituto de Física, Universidad Autónoma de Puebla, Apartado Postal J-48, Puebla, Puebla 72570, México*

²*Instituto de Física, Universidad Nacional Autónoma de México, Apartado Postal 20-364, México D.F. 01000, México*

*Corresponding author: upal@sirio.ifuap.buap.mx

Received May 8, 2008; accepted June 10, 2008;
posted June 26, 2008 (Doc. ID 95754); published July 30, 2008

Metal nanoshells, which consist of nanometer-scale dielectric cores surrounded by thin metallic shells, have been designed and studied for their linear optical responses. The plasmon resonance of metal nanoshells displays geometric tunability controlled by the ratio of shell thickness either to the core radius or to the total radius of the particle. Using Mie theory the surface plasmon resonance (SPR) of metallic nanoshells (Au, Ag, Cu) is studied for different geometries and physical environments. Considering a final radius of about 20 nm, the SPR peak position can be tuned from 510 nm (2.43 eV) to 660 nm (1.88 eV) for Au, from 360 nm (3.44 eV) to 560 nm (2.21 eV) for Ag, and from 553 nm (2.24 eV) to 655 nm (1.89 eV) for Cu, just by varying the ratio t/R_{Shell} and the environments inside and outside. With the decrease of the t/R_{Shell} ratio the SPR peak position gets redshifted exponentially and the shift is higher for a higher refractive index surroundings. The plasmon linewidth strongly depends on the surface scattering process and its FWHM increases with the reduction of shell thickness. © 2008 Optical Society of America

OCIS codes: 050.6624, 160.3900, 160.4236, 160.4760.

1. INTRODUCTION

Recently a considerable amount of research has been devoted to study the optical properties of metal nanoparticles. Of special interest is the controlled variation of the nanoparticle's geometry since this allows obtaining tunable optical properties that are not present in solid metallic particles [1]. A good example of such a strategy are metallic nanoshells (a dielectric core surrounded by a metallic shell), for which the structural tunability of the plasmon frequencies has been shown experimentally in a series of studies where monodispersed nanoshells of different thicknesses and core sizes have been fabricated and characterized with optical measurements [2–4]. The tunability of the plasmon position makes these nanoparticles particularly attractive for applications such as photo-oxidation inhibitors [5], all-optical switching devices [6,7], drug delivery [8], environmental sensors [9], and Raman sensors [10]. In spite of so much interest, there are few works in the literature [11,12] on the systematic study about the dependence of the optical response of metal nanoshells on their geometries and the surrounding medium.

In this work we used classical Mie calculations [13–15] to study linear optical properties of Au, Ag, and Cu nanoshells of different geometries. The effects of shell thickness, dielectric constants of core and dispersing media and core radius on the position, and intensity and linewidth of the surface plasmon resonance (SPR) are studied considering the effective dielectric constant of nanoshells of different metallic nanoshells (Au, Ag, and Cu). It has been demonstrated that the intensity, position,

and linewidth of the SPR peak can be tuned over a wide range just by manipulating the above mentioned parameters.

2. MIE THEORY

The Mie formulation consists in solving the classical electromagnetic equations for the interaction of a wave light with a metallic sphere [13]. These equations have an exact solution and several detailed deductions of this solution can be found in the literature [14,15]. In general terms, the method consists of finding the solutions for the Maxwell equations in spherical polar coordinates for an incident electromagnetic plane wave impinging on a metallic sphere with a radius R embedded in a medium with a refractive index n . The electromagnetic field is divided into two orthogonal subfields that can be deduced from a scalar potential. The solutions are expressed in terms of an infinite series where the coefficient constants are obtained from the appropriate boundary conditions at the surface of the sphere.

The interaction of light with metallic spheres produces scattering and absorption of the incident plane wave. The total energy loss of the incident radiation is the sum of the scattered and absorbed energies. These energy losses are expressed in a more convenient form by the cross sections that are a measure of the probability that an event (scattering, absorption, or extinction) will take place. The total extinction cross section σ_{ext} is given by $\sigma_{\text{ext}} = \sigma_{\text{sca}} + \sigma_{\text{abs}}$, where σ_{sca} and σ_{abs} are the scattering and absorption cross sections, respectively.

To express these cross sections for a metallic sphere according to the Mie formulation it is convenient to define the size parameter x and the relative refractive index m , given as

$$x = kR = \frac{2\pi nR}{\lambda}, \quad (1)$$

$$m = \frac{n_p}{n}, \quad (2)$$

where λ is the light wavelength in vacuum and n_p is the refractive index of the sphere. Here, k and mk represent the wavenumber in the dielectric medium and in the metallic sphere, respectively. For this case the cross sections are

$$\sigma_{\text{ext}} = \frac{2\pi}{k^2} \sum_{l=1}^{\infty} (2l+1) \text{Re}\{a_l + b_l\}, \quad (3)$$

$$\sigma_{\text{sca}} = \frac{2\pi}{k^2} \sum_{l=1}^{\infty} (2l+1) (|a_l|^2 + |b_l|^2), \quad (4)$$

$$\sigma_{\text{abs}} = \sigma_{\text{ext}} - \sigma_{\text{sca}}. \quad (5)$$

The coefficients a_l and b_l can be calculated by the expressions

$$a_l = \frac{\psi_l(y)[\psi_l'(m_2y) - A_l\chi_l'(m_2y)] - \psi_l'(y)[\psi_l(m_2y) - A_l\chi_l(m_2y)]}{\xi_l(y)[\psi_l'(m_2y) - A_l\chi_l'(m_2y)] - \xi_l'(y)[\psi_l(m_2y) - A_l\chi_l(m_2y)]}, \quad (9)$$

$$b_l = \frac{m_2\psi_l(y)[\psi_l'(m_2y) - B_l\chi_l'(m_2y)] - \psi_l'(y)[\psi_l(m_2y) - B_l\chi_l(m_2y)]}{m_2\xi_l(y)[\psi_l'(m_2y) - B_l\chi_l'(m_2y)] - \xi_l'(y)[\psi_l(m_2y) - B_l\chi_l(m_2y)]}, \quad (10)$$

where

$$A_l = \frac{m_2\psi_l(m_2x)\psi_l'(m_1x) - m_1\psi_l'(m_2x)\psi_l(m_1x)}{m_2\chi_l(m_2x)\psi_l'(m_1x) - m_1\chi_l'(m_2x)\psi_l(m_1x)}, \quad (11)$$

$$B_l = \frac{m_2\psi_l(m_1x)\psi_l'(m_2x) - m_1\psi_l(m_2x)\psi_l'(m_1x)}{m_2\chi_l'(m_2x)\psi_l(m_1x) - m_1\psi_l'(m_1x)\chi_l(m_2x)}, \quad (12)$$

$$x = kR_e, \quad y = kR_{sh}. \quad (13)$$

B. Dielectric Functions

In Mie's solution the problem is divided in two parts. The first one is the electromagnetic part, which is solved using first principles and is what we have described in Subsection 2.A. The second part is related with the material and can be solved using phenomenological dielectric functions $[\varepsilon(\omega, R)]$ that can be taken either from theoretical models

$$a_l = \frac{m\psi_l(mx)\psi_l'(x) - \psi_l'(mx)\psi_l(x)}{m\psi_l(mx)\xi_l'(x) - \psi_l'(mx)\xi_l(x)}, \quad (6)$$

$$b_l = \frac{\psi_l(mx)\psi_l'(x) - m\psi_l'(mx)\psi_l(x)}{\psi_l(mx)\xi_l'(x) - m\psi_l'(mx)\xi_l(x)}. \quad (7)$$

The functions ψ_l and ξ_l are the Riccati–Bessel functions defined as

$$\psi_l(z) = zj_l(z), \quad \xi_l(z) = zh_l(z), \quad (8)$$

where $j_l(z)$ are the spherical Bessel functions and $h_l(z)$ are the spherical Hankel functions [16,17]. The expressions ψ_l' and ξ_l' indicate differentiation with respect to the argument in parentheses. This Mie solution for the extinction by a single sphere also applies to any number of spheres when they have similar diameters and are randomly distributed with enough separations among them (distances larger than the incident wavelength). Under these circumstances coherent light is not scattered by the spheres and the total scattered energy is equal to the energy scattered by one sphere multiplied by their total number.

A. Core-Shell Structures

The original Mie formulation was extended by Aden and Kerker [18] in order to consider the scattering of light by a sphere with a concentric spherical shell embedded in a medium (core-shell structure), and they obtained new expressions to calculate the a_l and b_l coefficients [Eqs. (3)–(5) are still valid]:

or from experimental results. For the calculation of the optical response using Mie theory it is possible to use the dielectric functions measured experimentally for bulk metals, $\varepsilon_{\text{exp}}(\omega)$, as long as the appropriate size corrections are applied. These dielectric functions have contributions from interband and intraband transitions,

$$\varepsilon_{\text{exp}}(\omega) = \varepsilon_{\text{inter}}(\omega) + \varepsilon_{\text{intra}}(\omega). \quad (14)$$

In metals the electrons at the Fermi level can be excited by photons of very small energies, and therefore they are considered “free” electrons. The contributions from free electrons to $\varepsilon_{\text{exp}}(\omega)$ can be described by the Drude model [15],

$$\varepsilon_{\text{intra}}(\omega) = 1 - \frac{\omega_p^2}{\omega^2 + i\omega\Gamma}, \quad (15)$$

where ω_p is the plasma frequency and Γ is the damping constant arising from the dispersion of the electrons. Γ is

related with the mean free path of electrons (λ_e) by the expression $\Gamma = v_F/\lambda_e$, where v_F is the Fermi velocity.

Now we have to consider that electrons can also be dispersed by the nanoparticles (NP) surface, because the free electron's mean free path is now comparable or larger than the dimension of the particle. Therefore, it is necessary to modify the damping term to take into account the surface scattering of the free electrons,

$$\Gamma = \Gamma_{\text{bulk}} + \Gamma_R = \frac{v_F}{\lambda_e} + \frac{v_F}{R}. \quad (16)$$

From Eq. (14), we obtain the input of the bound charges by subtracting the free electron contribution from the bulk dielectric function. The free electron contributions are calculated using the Drude model [Eq. (15)] and ω_p is calculated by the expression $\omega_p = \sqrt{ne^2/\epsilon_0 m_{ef}}$, where n is the density of free electrons and m_{ef} is there effective mass. Now, we include the surface damping contribution by adding the extra damping term v_F/R to the Drude model and obtain the size-dependent dielectric function, which includes the contributions of the free electrons, surface damping, and interband transitions as

$$\begin{aligned} \epsilon(\omega, R) &= \epsilon_{\text{inter}}(\omega) + \epsilon_{\text{intra}}^{\text{NP}}(\omega, R) \\ &= \epsilon_{\text{exp}}(\omega) - \epsilon_{\text{intra}}(\omega) + \epsilon_{\text{intra}}^{\text{NP}}(\omega, R) \\ &= \epsilon_{\text{exp}}(\omega) + \frac{\omega_p^2}{\omega^2 + i\omega\Gamma_{\text{bulk}}} \\ &\quad - \frac{\omega_p^2}{\omega^2 + i\omega\left(\Gamma_{\text{bulk}} + \frac{v_F}{R}\right)}. \end{aligned} \quad (17)$$

Up to now we have considered a sphere of radius R where the surface damping is given by v_F/R . This correction can easily be extended to consider a shell if instead of the radius we consider its thickness (t): v_F/t . In both cases, the smaller the particle size (its radius or thickness) the more important is the surface dispersion effect. It has been shown that the surface dispersion effects do not change the location of the surface modes, but they affect the cou-

pling of such modes with the applied field, making the resonance peaks wider and less intense [19]. To show the effect of incorporating the dielectric function correction on the damping constant due to the surface dispersion effect, we calculated the damping constant for Cu clusters, which have a Fermi velocity of 1.57×10^6 m/s and a mean free path of electrons of 3.9×10^{-8} m [20]. While the $\Gamma_{\text{bulk}}^{\text{Cu}}$ has a value of $\sim 4.03 \times 10^{13}$ s $^{-1}$, for a Cu nanoshell of 5 nm thickness $\Gamma_{t=5 \text{ nm}}^{\text{Cu}}$ is $\sim 3.54 \times 10^{14}$ s $^{-1}$, which is 1 order of magnitude higher than the damping constant for the bulk material.

3. OPTICAL RESPONSE OF METALLIC NANOSHHELLS

A. Procedure

In this work we have considered and studied the nanoshells with geometries as shown in Fig. 1. Classical Mie calculations were performed in order to study the dependence of the SPR with the geometry for nanoshells of different metals (Au, Ag, and Cu) and different surrounding media (SiO $_2$, H $_2$ O, and vacuum). Among the three geometrical parameters of the nanoshells—the core radius (R_{Core}), the shell thickness (t), and the shell radius (R_{Shell})—only two are independent: $R_{\text{Shell}} = R_{\text{Core}} + t$. Nevertheless, it has been shown that the position of the SPR depends only on the t/R_{Shell} ratio [21]. In all the cases studied here we considered a vacuum core. For the numeric calculation of extinction spectra modifications proposed by Toon and Ackerman [22] were incorporated in the software to obtain better stability and accuracy of the results. We employed the bulk dielectric functions reported by Johnson and Christy [23] for silver, gold, and copper, which were modified according to Eq. (17) to incorporate the surface dispersion effects.

Three different cases were considered. In the first one, t was kept constant (5 nm) and R_{Core} was changed. For the second case, R_{Core} was fixed (10 nm) and t was changed. In the last case, R_{Shell} was kept constant (20 nm) while t and R_{Core} were changed simultaneously. In all the three cases the geometrical parameters were chosen in such ways that allowed us to cover the t/R_{Shell} ratio value between 0.2 and 0.8.

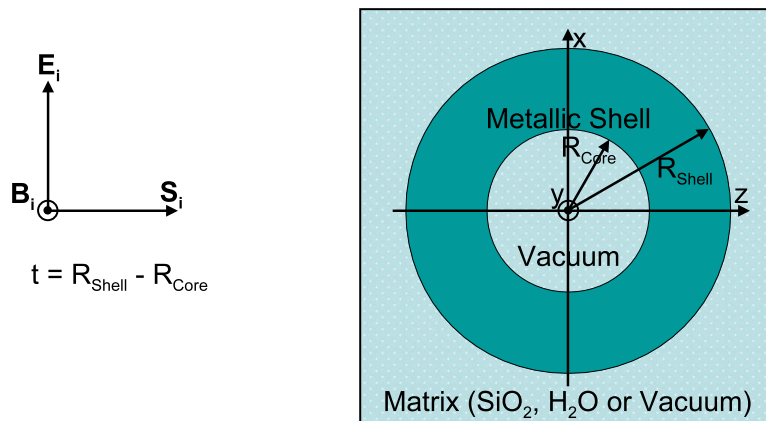


Fig. 1. (Color online) Schematic of the metal nanoshell geometries used for calculating linear optical properties.

B. Results

The optical extinction spectra obtained for the silver, gold, and copper nanoshells suspended–surrounded by vacuum, H₂O, and SiO₂ media are shown in the Figs. 2–4, respectively. For all the three systems, the FWHM of the SPR peak depended only on shell thickness t (inversely proportional). However, the intensity and position of the SPR peaks have a complex dependence on the shell thickness.

If the shell thickness is kept constant, the position of the SPR peak is redshifted when R_{Core} is increased. As an

example, for Au in vacuum [Fig. 3(a)] the position changed from 510.4 nm for a R_{Core} value of 1.3 nm to 576.0 nm for a R_{Core} value of 20.0 nm. Even bigger redshifts are obtained for the nanoshells embedded in a medium with a higher refractive index. For instance, for Au embedded in H₂O [$n=1.33$ [24]; Fig. 3(d)] the SPR peak shifts from 521.6 to 635.2 nm for the same values of R_{Core} than in the previous example. Similar results are obtained for the Ag and Cu nanoshells. In all the cases the intensity of the SPR peak increased for bigger R_{Core} values.

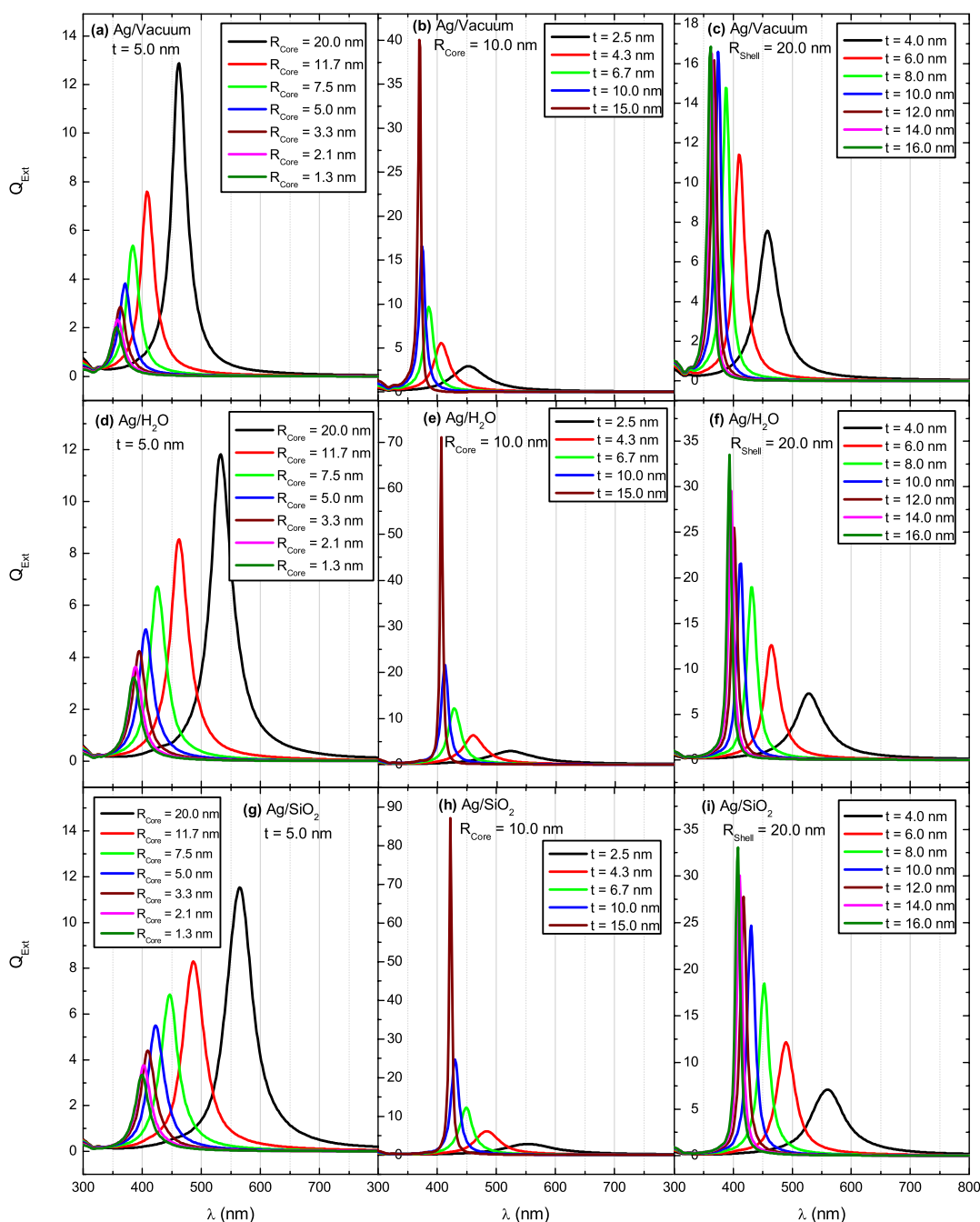


Fig. 2. (Color online) Simulated extinction spectra for Ag nanoshells (a) in vacuum, with constant thickness (5 nm) and varying R_{Core} ; (b) in vacuum, with constant R_{Core} (10 nm) and varying thickness; (c) in vacuum, with constant R_{Shell} (20 nm) and varying R_{Core} ; (d) in water, with constant thickness (5 nm) and varying R_{Core} ; (e) in water, with constant R_{Core} (10 nm) and varying thickness; (f) in water, with constant R_{Shell} (20 nm) and varying R_{Core} ; (g) in silica, with constant thickness (5 nm) and varying R_{Core} ; (h) in silica, with constant R_{Core} (10 nm) and varying thickness; (i) in silica, with constant R_{Shell} (20 nm) and varying R_{Core} .

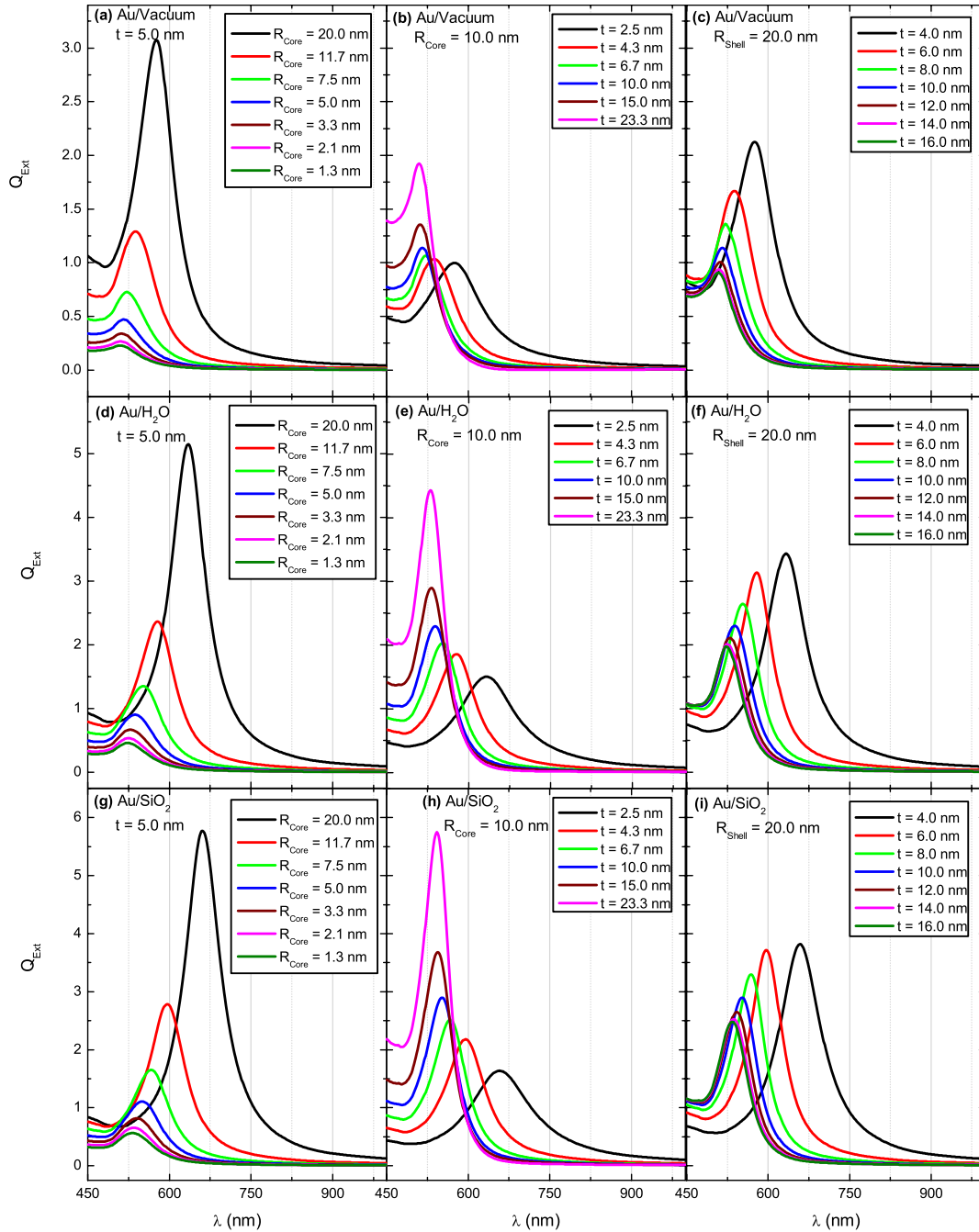


Fig. 3. (Color online) Simulated extinction spectra for Au nanoshells (a) in vacuum, with constant thickness (5 nm) and varying R_{Core} ; (b) in vacuum, with constant R_{Core} (10 nm) and varying thickness; (c) in vacuum, with constant R_{Shell} (20 nm) and varying R_{Core} ; (d) in water, with constant thickness (5 nm) and varying R_{Core} ; (e) in water, with constant R_{Core} (10 nm) and varying thickness; (f) in water, with constant R_{Shell} (20 nm) and varying R_{Core} ; (g) in silica, with constant thickness (5 nm) and varying R_{Core} ; (h) in silica, with constant R_{Core} (10 nm) and varying thickness, (i) in silica, with constant R_{Shell} (20 nm) and varying R_{Core} .

For the case when the core radius is constant important SPR redshifts are obtained by decreasing t . The magnitude of the shifts is proportional to the refractive index of the surrounding media. As for the intensity of the peaks, in general, it decreases for smaller shell thicknesses; however, there are some exceptions. For example, for Cu in vacuum [Fig. 4(b)] the intensity of the peak increases when we go from $t=4.3$ to 2.5 nm.

Finally, when the shell radius is constant ($t=20$ nm $-R_{\text{Core}}$), the higher redshifts are obtained for smaller val-

ues of t (bigger values of R_{Core}), which is in good agreement with the results of the two previous cases. The intensity is generally increased, but as in the previous case there are situations [for instance Ag in vacuum; Fig. 2(c)] when after a certain t/R_{Shell} value this tendency is reversed.

C. Discussion

To present the described results in a way that is easier to understand we graphed the variation of the positions

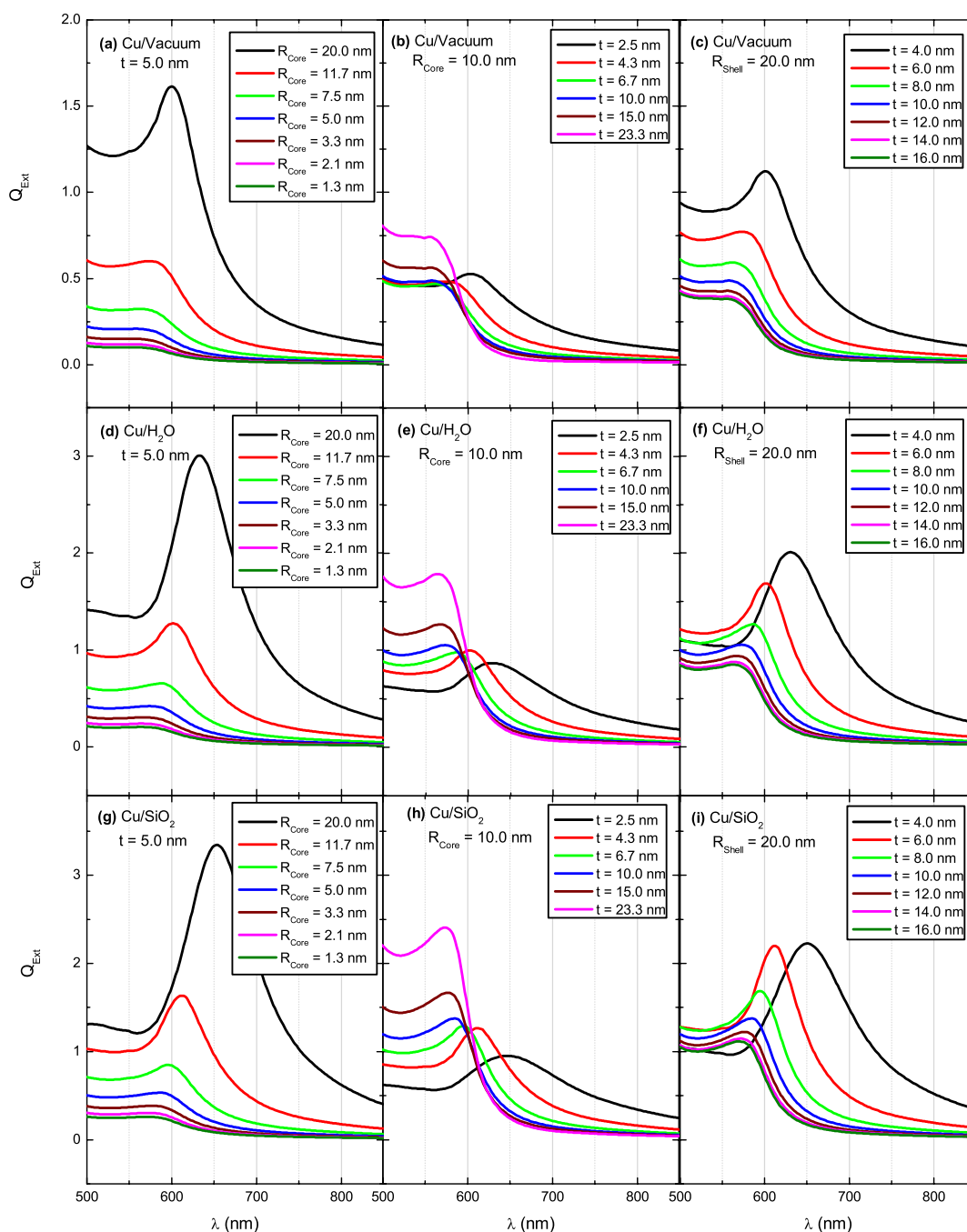


Fig. 4. (Color online) Simulated extinction spectra for Cu nanoshells (a) in vacuum, with constant thickness (5 nm) and varying R_{Core} ; (b) in vacuum, with constant R_{Core} (10 nm) and varying thickness; (c) in vacuum, with constant R_{Shell} (20 nm) and varying R_{Core} ; (d) in water, with constant thickness (5 nm) and varying R_{Core} ; (e) in water, with constant R_{Core} (10 nm) and varying thickness; (f) in water, with constant R_{Shell} (20 nm) and varying R_{Core} ; (g) in silica, with constant thickness (5 nm) and varying R_{Core} ; (h) in silica, with constant R_{Core} (10 nm) and varying thickness; (i) in silica, with constant R_{Shell} (20 nm) and varying R_{Core} .

(continuous curves) and intensities (dashed curves) of the obtained SPR peaks for Au, Ag, and Cu nanoshells with the t/R_{Shell} ratio (Fig. 5). From the figure it can be noted that as this ratio gets smaller than the unity (solid sphere), the SPR position gets redshifted exponentially and the shift is higher for a higher refractive index of the surrounding medium. This effect can be explained if we consider that the surface plasmon resonances of this system can be thought of in terms of a homogenous electron gas oscillating over a fixed positive background, with in-

duced surface charges providing the restoring force. When the surrounding medium is a dielectric, it polarizes in response to the resulting field, effectively reducing the strength of the surface charge and leading to a decreased restoring force and, consequently, lowering the plasmon energies. Although it was not considered in our calculations it is important to mention that the plasmon energies are further reduced if the nanostructures have an inner dielectric core, due to the same polarization effect in the inner frontier.

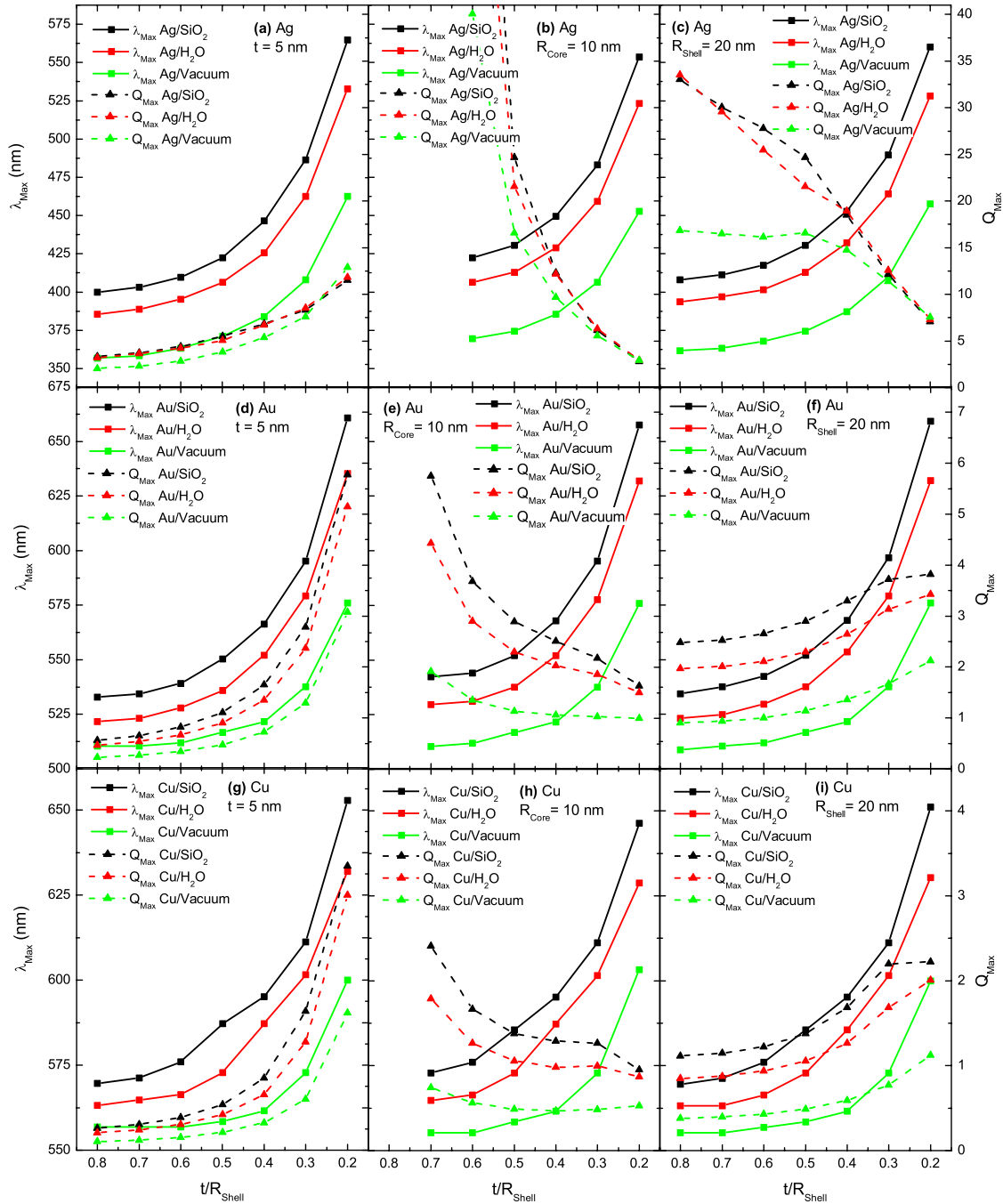


Fig. 5. (Color online) Summary of the SPR peak position (continuous curves) and intensity (dashed curves) behaviors for the Ag, Au, and Cu nanoshells (in rows) keeping the t , R_{Core} , and R_{Shell} (in columns) fixed.

The FWHM of the SPR peaks increases with the decrease of shell thickness as the result of reduced effective mean free path of the electrons (increase of collisions frequency) in the nanoshells. Though these surface dispersion effects do not change the location of the surface modes, they modify the interaction-coupling between the free electron vibrational modes and the applied field, making the resonance peaks wider and less intense. The effect is more pronounced for shell thickness below 5 nm.

In general the intensity of the SPR peak decreases as the t/R_{Shell} ratio gets smaller except at some critical points where the tendency is reversed. The exact value of the t/R_{Shell} ratio at the critical point is dependent on

metal and the thickness necessary to produce the shift. This behavior can be explained as the result of three competing phenomena: (a) if the SPR peak is in the region of interband transitions [for wavelengths below ~ 320.4 nm for Ag, ~ 496 nm for Au, and ~ 582.1 nm for Cu; Fig. (6)] a strong damping occurs, which is responsible for the decrease of intensity and the absorption background, therefore, when the position of the SPR is shifted outside this region the damping disappears and the peak gets considerably more intense; (b) the reduction in the shell thickness necessary to produce the SPR shift reduces the metal volume and because of this the intensity is decreased; and (c) As we explained in the previous paragraph, the reduc-

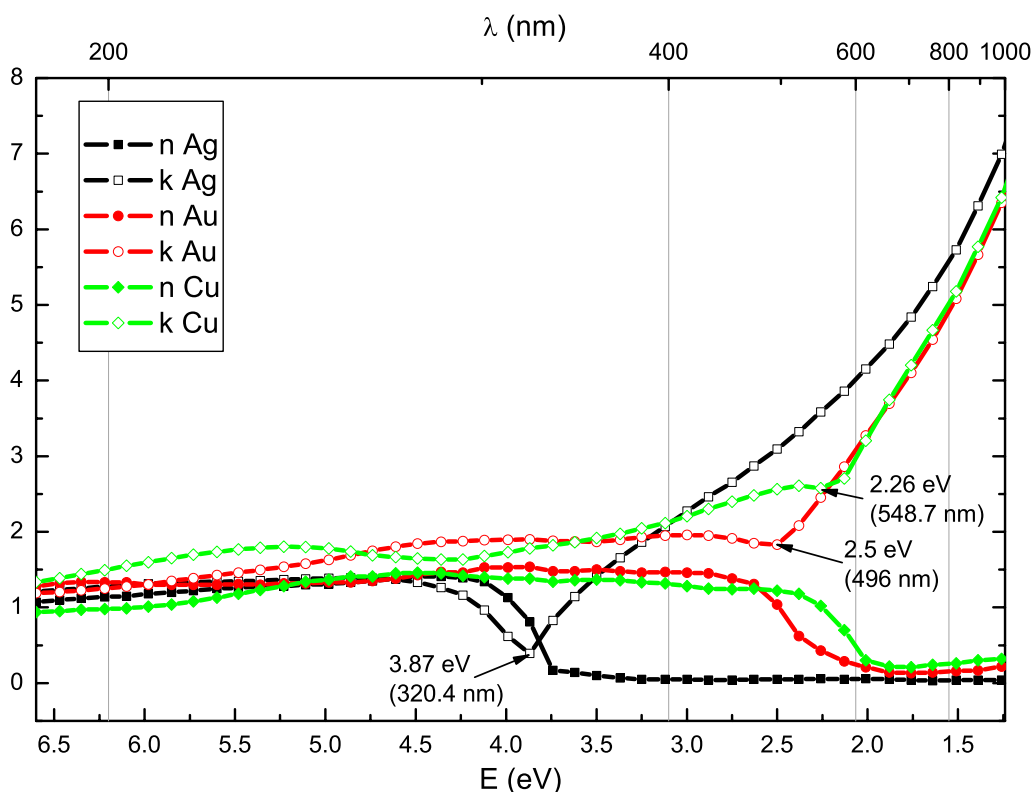


Fig. 6. (Color online) Bulk refractive index (experimental) of Ag (squares), Au (circles), and Cu (triangles) in the region of interest (from [23]).

tion of the effective mean free path of the electrons makes the SPR peak less intense. The first phenomenon is only of considerable importance when we pass the frontier from the region with interband transitions to the region without them and the other two phenomena are more important outside that region. That is why in general the SPR become less intense when we increase the t/R_{Shell} ratio. This behavior is better observed for Cu because the position of the SPR for the sphere is well into the region of interband transitions [25].

4. CONCLUSIONS

The Mie model is a first approximation to describe the optical response of metallic nanoshells. In this work we used this theory to calculate the optical extinction spectra of metallic nanoshells of three different metals embedded in different media and with varying geometric parameters. For all cases we showed that the intensity and position of the SPR peak strongly depends on the t/R_{Shell} ratio and explained the reasons for the observed variations.

We also showed that by manipulating the geometry of the metal nanostructures the SPR peak position and its intensity can be tailored in between a wide range of wavelengths to meet specific needs. So far there are few works in the literature showing those details and we consider that the results obtained in our calculations can save a lot of experimental work needed for the fabrication of metallic nanoshells for specific technological applications.

ACKNOWLEDGMENTS

The authors thank the anonymous reviewer for the useful comments and acknowledge the financial help of Consejo

Nacional de Ciencia y Tecnología (CONACyT), Mexico through the project 46269. O. Peña is grateful to CONACyT, Mexico for extending a postdoctoral fellowship.

REFERENCES

1. T. S. Ahmadi, Z. L. Wang, T. C. Green, A. Henglein, and M. A. El-Sayed, "Shape-controlled synthesis of colloidal platinum nanoparticles," *Science* **272**, 1924–1926 (1996).
2. R. D. Averitt, S. L. Westcott, and N. J. Halas, "Linear optical properties of gold nanoshells," *J. Opt. Soc. Am. B* **16**, 1824–1832 (1999).
3. S. J. Oldenburg, J. B. Jackson, S. L. Westcott, and N. J. Halas, "Infrared extinction properties of gold nanoshells," *Appl. Phys. Lett.* **75**, 2897–2899 (1999).
4. A. M. Schwartzberg, T. Y. Olson, Ch. E. Talley, and J. Z. Zhang, "Synthesis, characterization, and tunable optical properties of hollow gold nanospheres," *J. Phys. Chem. B* **110**, 19935–19944 (2006).
5. G. D. Hale, J. B. Jackson, O. E. Shmakova, T. R. Lee, and N. J. Halas, "Enhancing the active lifetime of luminescent semiconducting polymers via doping with metal nanoshells," *Appl. Phys. Lett.* **78**, 1502–1504 (2001).
6. S. Sershen, S. L. Westcott, J. L. West, and N. J. Halas, "An opto-mechanical nanoshell-polymer composite," *Appl. Phys. B* **73**, 379–381 (2001).
7. D. Ricard, P. Roussignol, and C. Flytzanis, "Surface-mediated enhancement of optical phase conjugation in metal colloids," *Opt. Lett.* **10**, 511–513 (1985).
8. S. Sershen, S. L. Westcott, N. J. Halas, and J. L. West, "Temperature-sensitive polymer-nanoshell composites for photothermally modulated drug delivery," *J. Biomed. Mater. Res.* **51**, 293–298 (2000).
9. Y. Sun and Y. Xia, "Increased sensitivity of surface plasmon resonance of gold nanoshells compared to that of gold solid colloids in response to environmental changes," *Anal. Chem.* **74**, 5297–5305 (2002).

10. J. B. Jackson, S. L. Westcott, L. R. Hirsch, J. L. West, and N. J. Halas, "Controlling the surface enhanced Raman effect via the nanoshell geometry," *Appl. Phys. Lett.* **82**, 257–259 (2003).
11. E. Prodan, A. Lee, and P. Nordlander, "The effect of a dielectric core and embedding medium on the polarizability of metallic nanoshells," *Chem. Phys. Lett.* **360**, 325–332 (2002).
12. E. Prodan, P. Nordlander, and N. J. Halas, "Effects of dielectric screening on the optical properties of metallic nanoshells," *Chem. Phys. Lett.* **368**, 94–101 (2003).
13. G. Mie, "Beiträge zur optik trüber medien, speziell kolloidaller metallösungen," *Ann. Phys.* **25**, 377–445 (1908).
14. M. Born and E. Wolf, *Principles of Optics*, 7th ed. (Cambridge U. Press, 1999).
15. C. F. Bohren and D. R. Huffman, *Absorption and Scattering of Light by Small Particles* (Wiley, 1983).
16. M. Abramowitz and I. A. Stegun, *Handbook of Mathematical Functions* (Dover, 1965).
17. G. Arfken, *Mathematical Methods for Physicists* (Academic, 1979).
18. A. L. Aden and M. Kerker, "Scattering of electromagnetic waves from two concentric spheres," *J. Appl. Phys.* **22**, 1242–1246 (1951).
19. C. Noguez, "Optical properties of isolated and supported metal nanoparticles," *Opt. Mater.* **27**, 1204–1211 (2005).
20. N. W. Ashcroft and N. D. Mermin, *Solid State Physics* (Holt–Saunders, 1976).
21. E. Prodan and P. Nordlander, "Structural tunability of the plasmon resonances in metallic nanoshells," *Nano Lett.* **3**, 543–547 (2003).
22. O. B. Toon and T. P. Ackerman, "Algorithms for the calculation of scattering by stratified spheres," *Appl. Opt.* **20**, 3657–3660 (1981).
23. P. B. Johnson and R. W. Christy, "Optical constants of the noble metals," *Phys. Rev. B* **6**, 4370–4379 (1972).
24. A. Curry, G. Nusz, A. Chilkoti, and A. Wax, "Substrate effect on refractive index dependence of plasmon resonance for individual silver nanoparticles observed using darkfield microspectroscopy," *Opt. Express* **13**, 2668–2677 (2005).
25. H. Wang, F. Tam, N. K. Grady, and N. J. Halas, "Cu nanoshells: effects of interband transitions on the nanoparticle plasmon resonance," *J. Phys. Chem. B* **109**, 18218–18222 (2005).